Machine Copy for Proofreading, Vol. x, y–z, 2014

Full-wave Analysis of Anisotropic Circular Microstrip Antenna with Air Gap Layer

Sami Bedra[1, *], Randa Bedra[1], Siham Benkouda[2], and Tarek Fortaki[1]

Abstract—In this paper, the effect of both uniaxial anisotropy in the substrate and air gap layer on the resonant frequency and bandwidth of circular microstrip patch are investigated. The problem is rigorously formulated based on the spectral domain technic in conjunction with Galerkin approach for computing the resonant frequency, half-power bandwidth, and radiation field of a tunable circular patch antenna which is printed on isotropic or uniaxial anisotropic substrate. The TM set of modes issued from the magnetic wall cavity model theory are used to expand the unknown currents on the patch. Resonant frequency shift due to uniaxial anisotropy is firstly investigated for different anisotropy ratio values of substrate. Then, the effect of inclusion of air gap layer inserted between anisotropic substrate and ground plane on the resonance characteristics is also investigated. The results obtained from this approach are in very good agreement with the experimental results available in the literature.

1. INTRODUCTION

Circular microstrip structure has been widely used in communication systems, wireless local area networks (WLANs) and some microwave applications radiator and resonators [1], due to their excellent advantages. Such advantages include small size, light weight, low production cost, conformal nature, and good aerodynamic characteristics [2]. Since the bandwidth of microstrip patch resonators and antennas around their operating frequencies is known to be very narrow, it is important to develop accurate algorithm for the computations of those resonant frequencies [3]. Many techniques of bandwidth enhancement have been suggested and design [4]. Bandwidth of microstrip antenna can be increased by designing the antenna with an air gap [1, 4]. In order to obtain tunable characteristics, providing a wider bandwidth at the same time, a simple solution was proposed in the literature [5–10]. This was the inclusion of an adjustable air gap between the ground plane and the substrate resulting in a two-layered structure having new resonant frequency value [7].

Various patch configurations implanted on different types of substrate have been tested and investigated [11]. In practice, it was found that the choice of the substrate material is of great importance and plays a significant role in achieving the optimum radiation characteristics of the antenna [12].

The circular microstrip patch printed on isotropic or anisotropic substrate has been analyzed extensively using the cavity model [13], analysis in the Fourier-Hankel transform domain [14], and the method of matched asymptotic expansion [15]. However, there is no theoretical report on the effect of both anisotropy in the substrate and the air gap, on the resonant characteristics of circular patch microstrip antenna by using spectral domain approach. These characteristics are firstly presented in this study by using spectral domain approach in conjunction with the Ritz-Galerkin's procedure.

This paper, is organized as follows, in Section 2, the analysis uses the full-wave formulation by means spectral domain approach in Galerkin's procedure for determining the resonant characteristics of air gap tuned anisotropic antenna. In Section 3, the validity of solution is tested by comparing the computed results with previously published data. The effect of uniaxial anisotropic in the substrate on

Received 22 December 2013

* Corresponding author: Sami Bedra (bedra_sami@hotmail.fr).

[1] Electronics Department, University of Batna, Batna 05000, Algeria. [2] Electronics Department, University of Constantine 1, Constantine 25000, Algeria.

the resonant frequency and half-power bandwidth of circular microstrip antenna with and without air gap are also investigated in this section. Finally, concluding remarks are summarized in Section 4.

2. SPECTRAL DOMAIN APPROACH FORMULATION

The patch is assumed to be located on a grounded dielectric slab of infinite extent, and the ground plane is assumed to be perfect electric conductor. The circular patch with radius a is printed on a substrate with dielectric constant, ε_r and thickness d_2, maintaining a variable air gap d_1 above the ground plane, (see Figure 1). All the dielectric materials are assumed to be nonmagnetic with permeability μ_0.

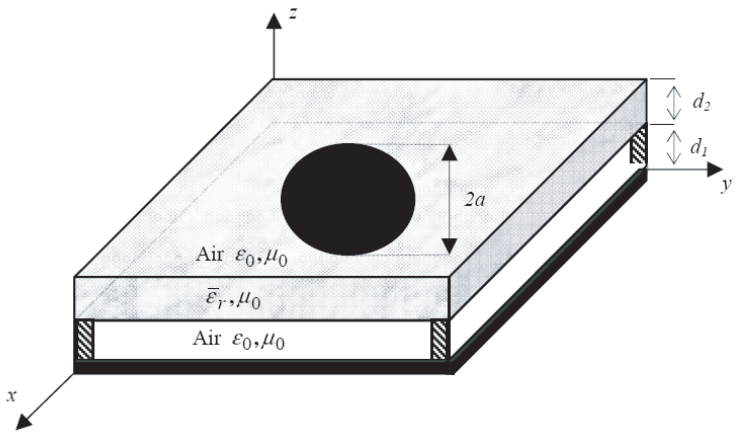

Figure 1. Geometry of suspended circular-disk microstrip antenna.

To simplify the analysis, the antenna feed will not be considered. In order to take the substrate uniaxial anisotropy's into account, the relative dielectric permittivity ε_r will be replaced with the tensor $\varepsilon_r = \text{diag}\ (\varepsilon_{rx}, \varepsilon_{ry}, \varepsilon_{rz})$, where ε_{rx} and ε_{rz} are the relative dielectric permittivity along x and z axis, respectively, (Figure 1).

In this work, our goal consists in taking into account the uniaxially anisotropic in the substrate and the air gap layer in the structure shown in Figure 1, without adding a supplementary complexity to the problem.

- For the case of isotropic substrate with air gap, the effective dielectric constant ε_{re} given in [10] is used to determine the effective dielectric thickness d_e. There resulting values are:

$$\varepsilon_{re} = \frac{\varepsilon_r \cdot (d_1 + d_2)}{(d_1 \cdot \varepsilon_r + d_2)} \tag{1}$$

$$d_e = d_2 + d_1 \tag{2}$$

- For the case of uniaxially anisotropic substrate, ε_{re} given in [16] there resulting values are:

$$\varepsilon_{re} = \varepsilon_z \tag{3}$$

$$d_e = d_2\sqrt{\frac{\varepsilon_x}{\varepsilon_z}} \tag{4}$$

The transverse fields inside the dielectric layer can be obtained via the inverse vector Hankel

transforms as [2, 17]

$$\mathbf{E}(\rho,\phi,z) = \begin{bmatrix} E_\rho(\rho,\phi,z) \\ E_\phi(\rho,\phi,z) \end{bmatrix} = \sum_{n=-\infty}^{n=+\infty} e^{in\phi} \int_0^\infty k_\rho dk_\rho \bar{\mathbf{H}}_n(\rho k_\rho) \cdot \mathbf{e}_n(k_\rho, z) \tag{5}$$

$$\mathbf{H}(\rho,\phi,z) = \begin{bmatrix} H_\phi(\rho,\phi,z) \\ -H_\rho(\rho,\phi,z) \end{bmatrix} = \sum_{n=-\infty}^{n=+\infty} e^{in\phi} \int_0^\infty k_\rho dk_\rho \, \bar{\mathbf{H}}_n(\rho k_\rho) \cdot \mathbf{h}_n(k_\rho, z) \tag{6}$$

$$\bar{\mathbf{H}}_n(\rho k_\rho) = \begin{bmatrix} J_n'(\rho k_\rho) & -\frac{in}{\rho k_\rho} J_n(\rho k_\rho) \\ \frac{in}{\rho k_\rho} J_n(\rho k_\rho) & J_n'(\rho k_\rho) \end{bmatrix} \tag{7}$$

In Eq. (7), $\bar{\mathbf{H}}_n(\rho k_\rho)$ is the kernel of the vector Hankel transform (VHT) [2, 17], $J_n(.)$ is the Bessel function of the first kind of order n, and the prime denotes differentiation with respect to the argument. The dagger implies conjugate transpose.

The relationship which relates the current on the conducting patch to the tangential electric field in the corresponding interface:

$$\mathbf{e}_n(k_\rho, z) = \bar{\mathbf{G}}(k_\rho) \cdot \mathbf{K}_n(k_\rho) \tag{8}$$

where $\bar{\mathbf{G}}(k_\rho)$ dyadic Green's function in the vector Hankel transform (VHT) domain [17]. Note that in the vector Hankel transform domain, the dyadic Green's function is diagonal and it is independent of the geometry of the radiating patch.

Note that, the tensor of Green for the considered structure can be easily determined. The tangential electric field is null on the conducting patch, which leads to an integral equation. To solve the integral equation, we apply the procedure of Galerkin which consists in developing the unknown distribution of the current on the circular patch is expanded into a series of basis functions [2, 17]. The basis functions chosen in this article for approximating the current density on the circular patch are obtained from the model of the cavity. Boundary conditions require that the transverse components of the electric field vanish on the perfectly conducting disk and the current vanishes off the disk, to give the following set of vector dual integral equations:

$$\mathbf{E}_n(\rho, z) = \int_0^{+\infty} dk_\rho k_\rho \bar{\mathbf{H}}_n(k_\rho \rho) \cdot \bar{\mathbf{G}}(k_\rho) \cdot \mathbf{k}_n(k_\rho) = 0, \quad \rho < a \tag{9}$$

$$\mathbf{K}_n(\rho) = \int_0^{+\infty} dk_\rho k_\rho \bar{\mathbf{H}}_n(k_\rho \rho) \cdot \mathbf{k}_n(k_\rho) = 0, \quad \rho > a \tag{10}$$

The use of the method of the moments in the spectral domain allows the resolution of the system of dual integral equations. The current on the disk is expressed in the form of a series of basis functions as follows:

$$\mathbf{K}_n(\rho) = \sum_{p=1}^{P} a_{np} \mathbf{\Psi}_{np}(\rho) + \sum_{q=1}^{Q} b_{nq} \mathbf{\Phi}_{nq}(\rho) \tag{11}$$

P and Q correspond to the number of basis functions of $\mathbf{\Psi}_{np}(\rho)$ and $\Phi_{nq}(\rho)$, respectively, a_{np} and b_{nq} are the mode expansion coefficients to be sought. The corresponding VHT of the current is given by

$$\mathbf{K}_n(k\rho) = \sum_{p=1}^{P} a_{np} \mathbf{\Psi}_{np}(k\rho) + \sum_{q=1}^{Q} b_{nq} \mathbf{\Phi}_{nq}(k\rho) \tag{12}$$

Substitute the current expansion (12) into (8). Next, multiplying the resulting equation by $\rho \mathbf{\Psi}_{nk}^{+}(\rho)$ $(k = 1, 2, \ldots, P)$ and by $\rho \mathbf{\Phi}_{nl}^{+}(\rho)$ $(l = 1, 2, \ldots, Q)$, and while integrating from 0 to a,

and using the Parseval's theorem for vector Hankel transform [2], we obtain a system of linear $P+Q$ algebraic equations for each mode n which can be written in the matrix form:

$$\bar{\mathbf{Z}}_n \cdot \mathbf{C}_n = 0 \tag{13}$$

$$\bar{\mathbf{Z}}_n = \begin{bmatrix} \left(\bar{\mathbf{Z}}_n^{\mathbf{\Psi\Psi}} n\right)_{P\times P} & \left(\bar{\mathbf{Z}}_n^{\mathbf{\Psi\Phi}}\right)_{P\times Q} \\ \left(\bar{\mathbf{Z}}_n^{\mathbf{\Phi\Psi}} n\right)_{Q\times P} & \left(\bar{\mathbf{Z}}_n^{\Phi\Phi} n\right)_{Q\times Q} \end{bmatrix}, \qquad \mathbf{C}_n = \begin{bmatrix} (\mathbf{a}_n)_{p\times 1} \\ (\mathbf{b}_n)_{q\times 1} \end{bmatrix} \tag{14}$$

Each element of the submatrices is given by:

$$\bar{\mathbf{Z}}_n^{\mathbf{VW}}(i,j) = \int_0^{+\infty} dk\rho \mathbf{V}_{ni}^{+}(k_\rho) \cdot \bar{\mathbf{G}}(k_\rho) \cdot \mathbf{W}_{nj}(k_\rho) \tag{15}$$

where $\mathbf{V}$ and $\mathbf{W}$ represent either $\mathbf{\Psi}$ or $\mathbf{\Phi}$. For every value of the integer n, the system of linear Equations (15) has non-trivial solutions when

$$\det\left[\bar{\mathbf{Z}}_n(\omega)\right] = 0 \tag{16}$$

This Equation (16) is called characteristic equation of the structure (Figure 1). For the search of the complex roots of this equation, the method of Müller is used.

It requires three initial guesses which must be close if possible to the sought solution to ensure a fast convergence.

Generally the real part (f_r) of the solution represents the resonant frequency of the structure, the imaginary part (f_i) indicates the losses of energy per radiation and the ratio ($2f_i/f_r$) gives the band-width (BW) and the quantities $Q = (f_r/2f_i)$ stands for the quality factor [2].

3. NUMERICAL RESULTS AND DISCUSSION

In order to confirm the computation accuracy of the spectral domain approach, our results are compared with experimental and recent theoretical data [18–20]. Experimental and numerical evaluations have been performed with a patch for different radius a, printed on single substrate ($d_1 = 0$) with relative permittivity $\varepsilon_r = 2.43$ and thickness $d_2 = 0.49\,\text{mm}$.

The Table 1 summarizes our computed resonant frequencies and those obtained for TM^{11} mode via spectral domain formulation [18–20]. The comparisons show a good agreement between our results and those of literature [18–20].

Table 1. Theoretical and experimental values of the resonant frequency for the fundamonatl mode of circular microstrip antennas without air gap. $d_1 = 0$, $\varepsilon_r = 2.43$, $d_2 = 0.49\,\text{mm}$.

a (mm)	a/h	Experiment (GHz) [18]	Computed (GHz)			
			[18]	[19]	[20]	Present
1.9698	4.02	25.60	25.30	25.92	25.40	25.66
3.9592	8.08	13.10	13.30	13.55	13.30	13.26
5.8898	12.02	8.960	9.13	9.25	9.20	9.020
8.0017	16.33	6.810	6.80	6.87	—	6.816
9.9617	20.33	5.470	5.49	5.54	5.60	5.504

In order to check the accuracy of the spectral domain method described in the previous section for two-layered case, our results are compared with an experimental and theoretical values presented in the previous work [19].

In Table 2, our calculated resonant frequencies and bandwidth are compared with measured results [19], for the tunable circular microstrip patch shown in Figure 1. The agreement between the calculated and measured results is good for different values of air gap separation.

Table 2. Comparison of measured and calculated resonant frequency and half-power bandwidth for a circular microstrip patch with different thickness of air gap d_1, $a = 50\,\text{mm}$, $\varepsilon_r = 2.32$, $d_2 = 1.5748\,\text{mm}$.

Resonant frequency f_r^{11} (GHz), Bandwidth BW (%)						
d_1 (mm)	Measured [19]		Calculated [19]		Our calculation	
	f_r^{11}(GHz)	BW (%)	f_r^{11} (GHz)	BW (%)	f_r^{11} (GHz)	BW (%)
0.5	1.262	1.632	1.272	1.457	1.283	1.537
1	1.368	2.018	1.339	1.954	1.365	2.075
2	1.462	3.122	1.398	2.911	1.437	3.082
3	1.50	4.208	1.417	3.848	1.465	4.041
4	1.530	4.50	1.420	4.778	1.475	4.882

Figure 2 shows the resonant frequency against the air gap thickness for various radius of the circular-disk patch. It is seen that the operating frequency increases with the air layer thickness for a given value of patch size, however, it depends inversely on the patch size for a given air gap width d_1.

The radiation pattern of circular microstrip antenna is showen in Figure 3 for different values of the air gap thickness. It is verified that an increases in the air gap thickness improves the directivity of the antenna.

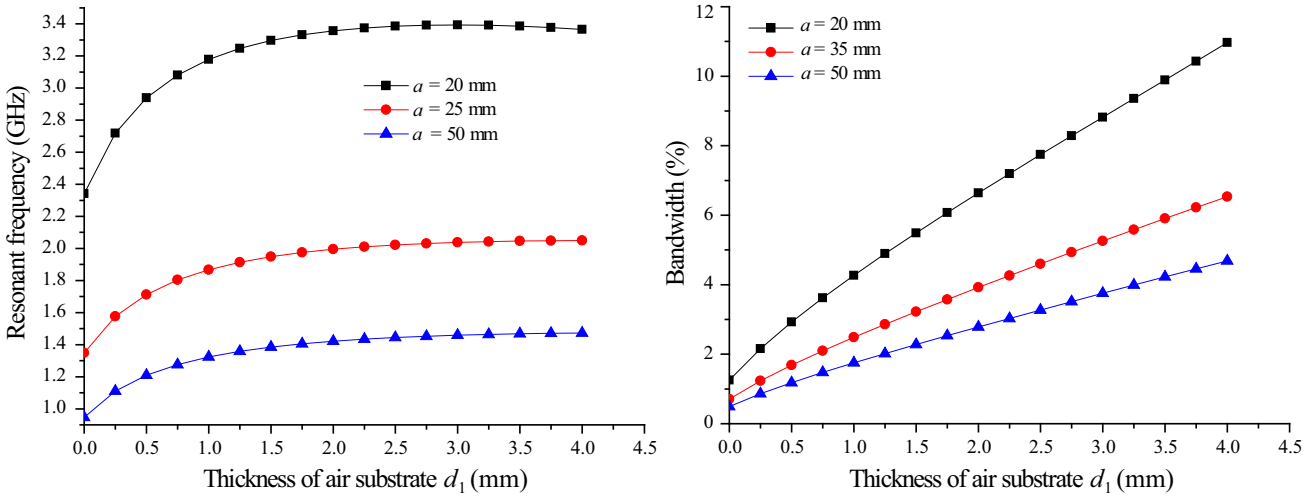

Figure 2. (a) Resonant frequency and (b) bandwidth of circular microstrip antenna versus air gap thickness for different values of patch radius; $\varepsilon_r = 3.4$, $d_2 = 1.27\,\text{mm}$.

Next, the effect of uniaxial anisotropy on the resonant frequency is analyzed. The anisotropy ratio (AR) is defined as

$$AR = \varepsilon_x/\varepsilon_z \tag{17}$$

The resonant frequency of a circular microstrip patch antenna with radius $a = 5\,\text{mm}$, and substrate thickness $d_2 = 1.27\,\text{mm}$, for different pairs of relative permittivities (ε_x, ε_z) is depicted in Table 3. The change in the resonant frequency relative to the isotropic case ($\varepsilon_x = \varepsilon_z = 3.4$) is calculated using the following expression:

$$\frac{\Delta f_r}{f_r} = \left|1 - \frac{f_{ra}}{f_{ri}}\right| \tag{18}$$

where f_{ri} and f_{ra} are, respectively, the resonant frequencies of the antenna for the isotropic and uniaxial anisotropic cases. We observe that, for negative uniaxial anisotropy with $AR = 2$, the resonant frequency f_{ri}, can shift to a lower value of f_r (8.284 GHz) or higher frequency of (11.212 GHz). A similar remark

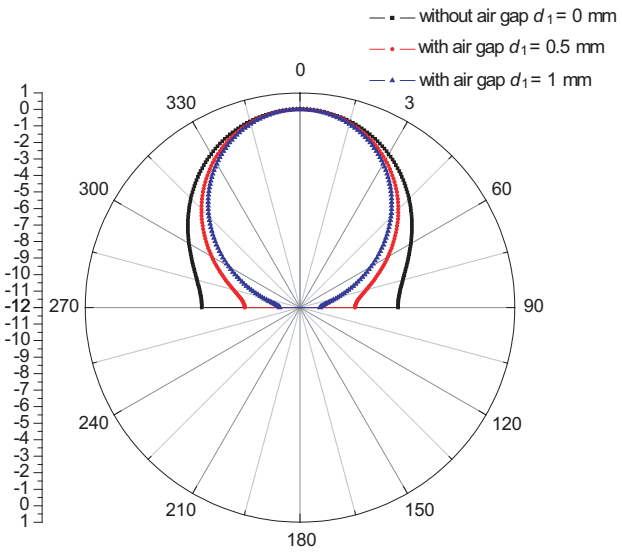

Figure 3. Radiation pattern (E plane) versus air gap thickness; $a = 50\,\text{mm}$, $d_2 = 1.59\,\text{mm}$, $\varepsilon_r = 2.32$.

Table 3. Dependence of the resonant frequency for the fundamental mode of circular microstrip antennas without air gap on relative permittivities (ε_x, ε_z); $a = 5\,\text{mm}$, $d_1 = 0$, $d_2 = 1.27\,\text{mm}$.

Uniaxial Anisotropy type	Relative permittivity		Anisotropic ratio AR	Resonant frequency (GHz)	Fractional Change $\frac{\Delta f_r}{f_r}(\%)$
	ε_x	ε_z	$AR = \varepsilon_x/\varepsilon_z$	f_r^{11}	
Isotropic	3.4	3.4	1	8.636	0
Negative	6.8	3.4	2	8.284	4.08
Negative	3.4	1.7	2	11.212	29.83
Positive	1.7	3.4	0.5	8.899	3.05
Positive	3.4	6.8	0.5	6.437	25.46

can be made for the positive uniaxial anisotropy case with $AR = 0.5$; the corresponding values of lower and higher frequencies are, respectively, (6.437 GHz) and (8.899 GHz). Consequently, the AR parameter alone is not sufficient to enhance a decision about whether there is an increase or decrease in resonant frequency to be made.

The resonant frequencies and half-power bandwidth of the circular patch for different air gap thicknesses against the substrate thickness are shown in Figures 4(a) and (b), where isotropic ($\varepsilon_x = \varepsilon_z = 5.12$), negative ($\varepsilon_x > \varepsilon_z$) uniaxial anisotropic and positive ($\varepsilon_x < \varepsilon_z$) uniaxial anisotropic substrates are considered.

In Figure 4(a), the anisotropy is obtained by changing ε_z while keeping ε_x constant. The effect of the permittivity along the optical axis persists for low as well as for high substrate thicknesses.

When ε_x is changed and ε_z remains constant, the influence of the resonant frequency decreases with reductions in substrate thickness as shown in Figure 4(b). This influence tends to be neglected for lower substrate thickness. These behaviors agree very well with those reported for a various shapes patch antenna, by [7, 8, 10, 11]. We can conclude that the permittivity ε_z along the optical axis is the significant and most important factor in determination of the resonant frequency.

Figures 5(a) and (b) depict the influence of the air gap thickness on the resonant frequency and half-power bandwidth of circular microstrip patch for three anisotropic dielectric substrates: Boron

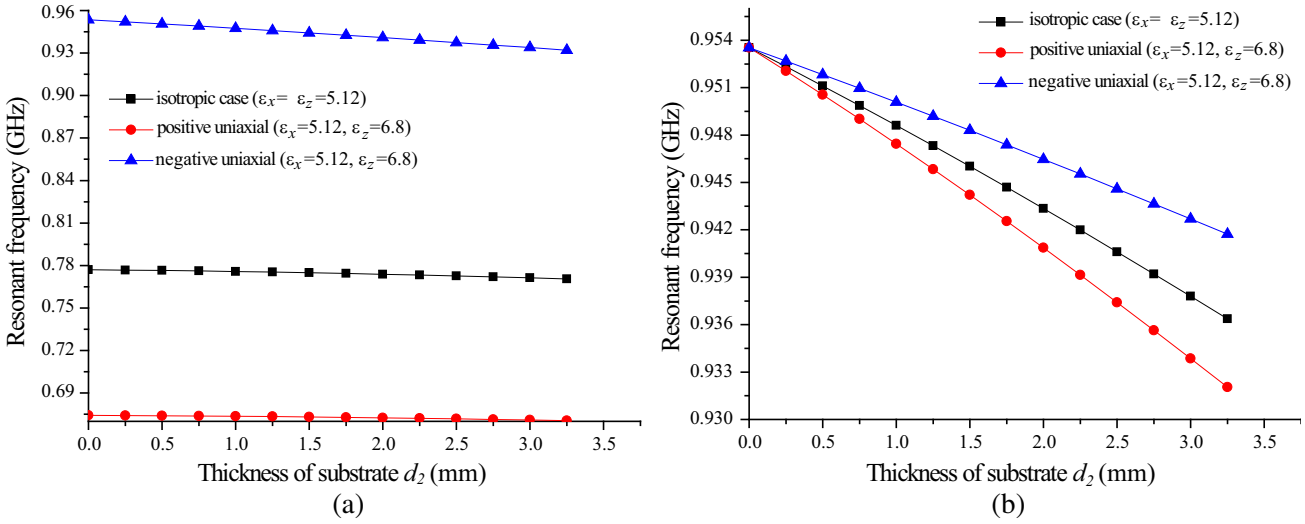

Figure 4. Resonant frequency versus substrate thicknesses for different permittivity pairs (ε_x, ε_z); (a) When ε_z changed, (b) when ε_x changed, with $d_1 = 0\,\text{mm}$, $a = 50\,\text{mm}$.

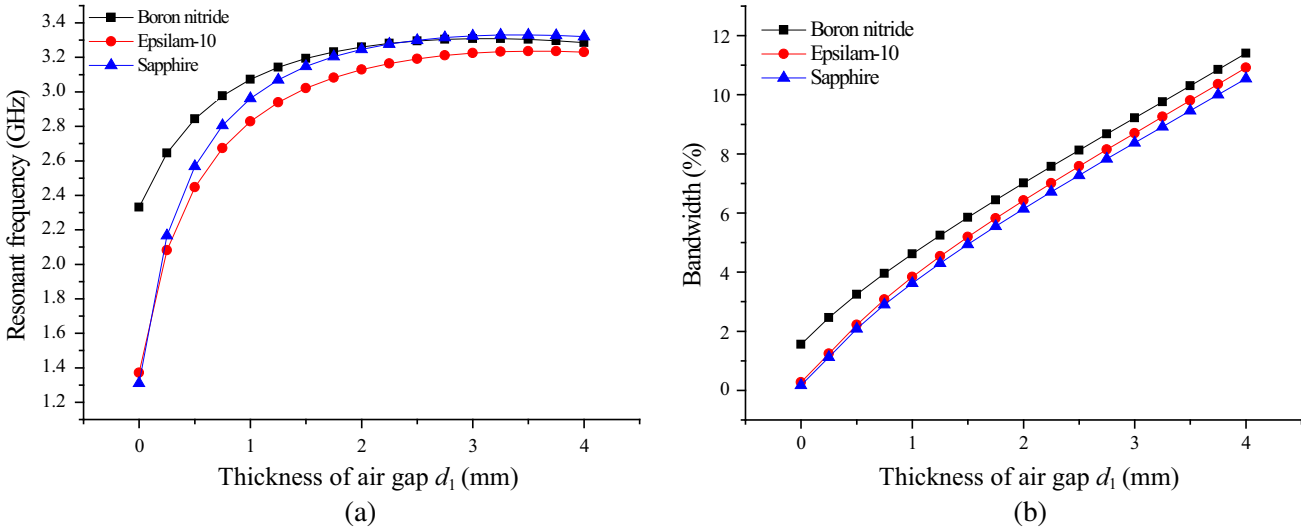

Figure 5. (a) Resonant frequency and (b) bandwidth versus air gap thickness for different anisotropic substrates; $a = 20\,\text{mm}$, $d_2 = 1.27\,\text{mm}$.

nitride ($\varepsilon_z = 3.4$, $\varepsilon_x = 5.12$) Epsilam-10 ($\varepsilon_z = 10.3$, ε_x =13), and Sapphire ($\varepsilon_z = 11.6$, $\varepsilon_x = 9.4$). The substrate has thickness $d_1 = 1.59\,\text{mm}$ and the air gap width is varied from 0 mm to 4 mm.

As it can be seen, the resonant frequency reduces considerably when the dielectric substrate changes from Boron nitride to epsilam-10, and this is in contrast to what happens when the medium changes from Epsilam-10 to Sapphire. A similar remark can be made for the half-power bandwidth of circular microstrip antenna with air gap for different anisotropic dielectric substrates.

In Figure 6, we present the influence of uniaxial anisotropy in the substrate on the radiation pattern of circular microstrip antenna with the isotropic, positive uniaxial anisotropic and negative uniaxial anisotropic substrate are considered. It is observed that the directivity of the antenna is considerably affect when the permittivity along the optical axis (ε_z) changed and (ε_x) remained constant (Figure 6(a)). On the other hand uniaxial anisotropy does not have a considerably effect on the radiation pattern of the circular antenna when the permittivity perpendical to the optical axis (ε_x) changed and (ε_z) remained constant (Figure 6(b)).

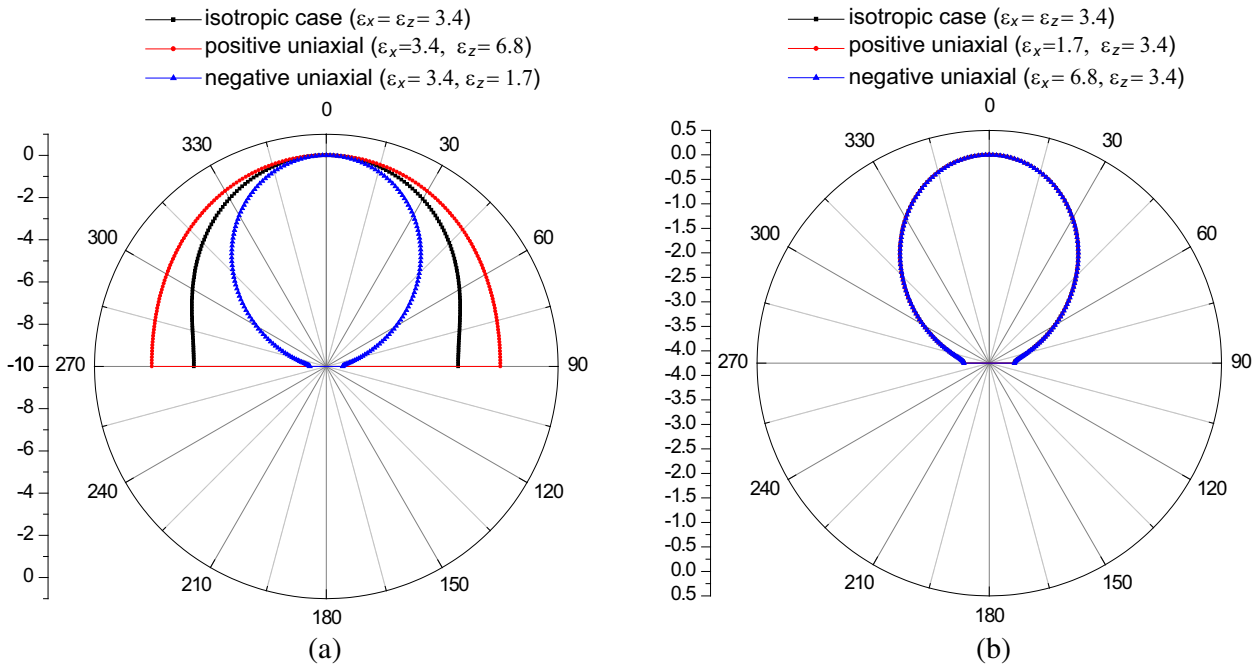

Figure 6. Radiation pattern (E plane) versus the angle theta for the isotropic, positive uniaxial anisotropic and negative uniaxial anisotropic substrates. (a) When changing ε_z, (b) when changing ε_x.

4. CONCLUSION

In this paper, a full-wave analysis has been applied to investigate the effect of suspended and the uniaxial anisotropy substrate on the radiation characteristics of a circular microstrip antenna. The spectral-domain integral equation in conjunction with stationary phase method have been used to calculate the complex resonant frequency and radiation pattern of various antenna structures. In order to test the validity of the analysis, the numerical results obtained via Galerkin's method have been compared with theoretical and experimental data, and good agreement has been found. Numerical results for the resonant frequency, half-power bandwidth and radiation pattern have been presented for various patch configurations, including cases of a patch on a single anisotropic layer, a patch on a double layer with one layer anisotropic and one layer isotropic (suspended patch). Computations show that the air separation can be adjusted to have the maximum operating frequency of the antenna. The bandwidth, on other hand increases monotonically with increasing the air gap width. Furthermore, the resonant frequency, half-power bandwidth and radiation field of a circular microstrip patch antenna are sensitive to the variations of the permittivity of a uniaxial anisotropic substrate along the optical axis (ε_z). The results of the study will also be useful in the circular microstrip design using uniaxial metamaterials.

REFERENCES

1. Gürel, C. S. and E. Yazgan, "Resonant frequency of air gap tuned circular microstrip antenna with anisotropic substrate and superstrate layers," *Journal of Electromagnetic Waves and Applications*, Vol. 24, No. 13, 1731–1740, 2010.
2. Fortaki, T., D. Khedrouche, F. Bouttout, and A. Benghalia, "Vector Hankel transform analysis of a tunable circular microstrip patch," *Commun. Numer. Meth. Engng.*, Vol. 21, 219–231, 2005.
3. Fortaki, T., S. Benkouda, M. Amir, and A. Benghalia, "Air gap tuning effect on the resonant frequency and half-power bandwidth of superconducting microstrip patch," *PIERS Online*, Vol. 5, No. 4, 350–354, 2009.
4. Barkat, O., "Theoretical investigation of an air gap tuned superconducting annular ring microstrip antenna," *International Conference on Complex Systems (ICCS)*, 1–5, 2012.

5. Lee, K. F. and J. S. Dahele, "Circular-disk microstrip antennas with an air gaps," *IEEE Transactions on Antennas and Propagation*, Vol. 32, No. 8, 880–884, Aug. 1984.
6. Abboud, F., J. P. Damiano, and A. Papiernik, "A new model for calculating the input impedance of coax-fed circular microstrip antennas with and without air gap," *IEEE Transactions on Antennas and Propagation*, Vol. 38, No. 11, 1882–1885, 1990.
7. Gurel, C. S. and E. Yazgan, "Resonant frequency of an air gap tuned circular disk microstrip antenna," *Int. J. Electron.*, Vol. 87, 973–979, 2000.
8. Guha, D., "Resonant frequency of circular microstrip antennas with and without air gaps," *IEEE Transactions on Antennas and Propagation*, Vol. 49, No. 1, 55–59, 2001.
9. Gunel, T., "Continuous hybrid approach to the modified resonant frequency calculation for circular microstrip antennas with and without air gaps," *Microwave Opt. Tech. Lett.*, Vol. 40, 423–427, 2004.
10. Gurel, C. S., E. Aydın, and E. Yazgan, "Computation and optimization of resonant frequency and input impedance of a coax-fed circular patch microstrip antenna," *Microwave Opt. Tech. Lett.*, Vol. 49, No. 9, 2263–2267, Sep. 2007.
11. Bedra, S., S. Benkouda, M. Amir, and T. Fortaki, "Resonant frequency of tunable microstrip ring antenna printed on isotropic or uniaxially anisotropic substrate," *Advanced Electromagnetics*, Vol. 2, No. 2, 6–9, 2013.
12. Djouablia, L., I. Messoudan, and A. Benghalia, "Uniaxial anisotropic substrate effect on the resonance of an equitriangular microstrip patch antenna," *Progress In Electromagnetics Reaserch M*, Vol. 24, 45–56, 2012.
13. Verma, A. K. and Nasimuddin, "Multilayer cavity model for microstrip rectangular and circular patch antenna," *Electromagnetics*, Vol. 24, No. 3, 193–217, 2004.
14. Chew, W. C. and J. A. Kong,, "Analysis of a circular microstrip disk antenna with a thick dielectric substrate," *IEEE Transactions on Antennas and Propagation*, Vol. 29, No. 1, 68–76, Jan. 1981.
15. Gurel, C. S. and E. Yazgan, "Characteristics of a circular patch microstrip antenna on a uniaxially anisotropic substrate," *IEEE Transactions on Antennas and Propagation*, Vol. 52, No. 10, 2532–2537, 2004.
16. Tighilt, Y., F. Bouttout, and A. Khellaf, "Modeling and design of printed antennas using neural networks," *Int. J. RF and Microwave CAE*, Vol. 21, 228–233, 2011.
17. Chew, W. C. and T. M. Habashy, "The use of vector transforms in solving some electromagnetic scattering problems," *IEEE Transactions on Antennas and Propagation*, Vol. 34, No. 7, 871–879, 1986.
18. Losada, V., R. R. Boix, and M. Horn, "Resonant modes of circular microstrip patches in multilayered substrate," *IEEE Transactions on Antennas and Propagation*, Vol. 47, No. 4, 488–497 Apr. 1999.
19. Benmeddour, F., C. Dumond, F. Benabdelaziz, and F. Bouttout, "Improving the performances of a high Tc superconducting circular microstrip antenna with multilayered configuration and anisotropic," *Progress In Electromagnetics Research C*, Vol. 18, 169–183, 2011.
20. Motevasselian, A., "Spectral domain analysis of resonant charcteristics and radiation patterns of a circular disc and an annular ring microstrip antenna on uniaxial susbtrate," *Progress In Electromagnetics Research M*, Vol. 21, 237–251, 2011.